Space charge limited current emission for a sharp tip

Cite as: Phys. Plasmas **22**, 052106 (2015); https://doi.org/10.1063/1.4919936
Submitted: 02 March 2015 • Accepted: 22 April 2015 • Published Online: 08 May 2015

Y. B. Zhu and L. K. Ang

Space charge limited current emission for a sharp tip

Y. B. Zhu[a] and L. K. Ang[b]
Engineering Product Development, Singapore University of Technology and Design, Singapore 487372

(Received 2 March 2015; accepted 22 April 2015; published online 8 May 2015)

In this paper, we formulate a self-consistent model to study the space charge limited current emission from a sharp tip in a dc gap. The tip is assumed to have a radius in the order of 10s nanometer. The electrons are emitted from the tip due to field emission process. It is found that the localized current density J at the apex of the tip can be much higher than the classical Child Langmuir law (flat surface). A scaling of $J \propto V_g^{3/2}/D^m$, where V_g is the gap bias, D is the gap size, and $m = 1.1$–1.2 (depending on the emission area or radius) is proposed. The effects of non-uniform emission and the spatial dependence of work function are presented. © *2015 AIP Publishing LLC*. [http://dx.doi.org/10.1063/1.4919936]

I. INTRODUCTION

Space-charge-limited (SCL) electron flow is the maximum current density allowed to be transported across a spacing D with a potential difference V_g. The first SCL current model was formulated about 100 years ago[1,2] by Child and Langmuir (CL) for a planar electrode

$$J_{CL} = \frac{4}{9}\varepsilon_0\sqrt{\frac{2e}{m}}\frac{V_g^{3/2}}{D^2}, \tag{1}$$

where e and m are, respectively, the charge and mass of the electron, and ε_0 is the permittivity of free space. Due to the contemporary needs on the studies of nanogaps and short electron bunches, this 1D classical CL law has been extended to various regimes, including multi-dimensions,[3–7] quantum regime,[8,9] short pulse limit,[10,11] single-electron limit,[12] new scaling in other geometries[13] with applications in THz source[14,15] and time dependent current injection.[16–18] Electron emission from a sharp tip is important for many applications, such as vacuum microelectronics,[19] compact high current cathodes for high power microwave sources,[20–22] ultrafast laser induced electron emission from sharp tip,[23–27] ultrafast electron imaging,[28–30] laser-driven dielectric acceleration,[31,32] and high brightness photo-cathode[33,34] for X-ray free electron laser (FEL).

For electron emission from a sharp tip, the localized electron density near to the tip is very high, which induces a space charge electric field, strong enough to modify the external applied electric field significantly, and thus to influence the field emission process. The classical CL law [Eq. (1)] is not sufficient to address this problem, as it has ignored the sharpness of the tip, which may induce non-uniform emission from the tip. While there were models dealing with the transition from field emission to CL law, these models[35–38] remained to be one-dimensional and inconsistent, as the sharpness of the tip was ignored completely. In this paper, we construct a model to study the space charge limited current emission for a sharp tip.

II. MODEL

In Fig. 1(a), we consider a sharp tip of radius R that is approximated as a hyperboloid emitter, which has a cylindrical symmetry about the z-axis.[39,40] It is expressed in the prolate spheroidal coordinates $(u, v,$ and $\varphi)$

$$x = a\sinh(u)\sin(v)\cos(\varphi), \tag{2a}$$

$$y = a\sinh(u)\sin(v)\sin(\varphi), \tag{2b}$$

$$z = a\cosh(u)\cos(v), \tag{2c}$$

where a is one-half of the distance between the hyperbolic foci, u is a nonnegative number, $v \in [0, \pi]$, and $\varphi \in [0, 2\pi]$. The apex of the tip is located at a distance of D with a potential difference of V_g. The tip half angle θ is calculated by $\cos^2\theta = D/(D+R)$ for $D = 0.1$–$1\ \mu$m, and $R = 50$–200 nm. The parameter a can be calculated using $a = D/\cos(\theta)$. Unless it is specified elsewhere, the default values are $R = 50$ nm and $D = 1\ \mu$m.

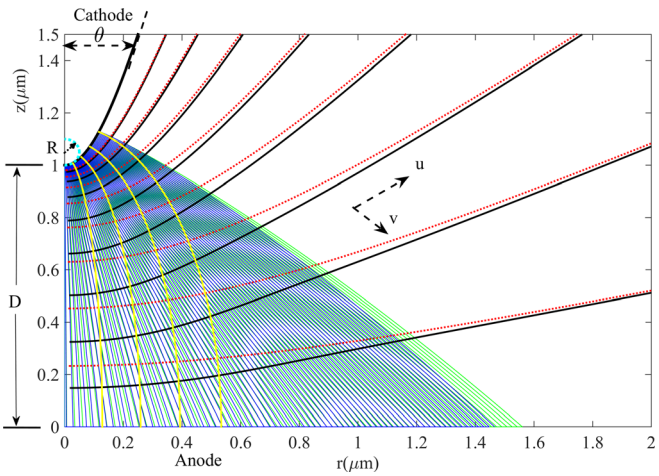

FIG. 1. Electron trajectories (blue and green) and equal potentials (dotted red line and solid black): green and black (red and blue) lines are calculation with (without) the space charge effect. The yellow curve is the vacuum electric field line, which is orthogonal with the dotted red line. The parameters are $R = 50$ nm, $D = 1\ \mu$m, and $V_g = 2$ kV.

[a]zhuyingbin@gmail.com
[b]ricky_ang@sutd.edu.sg

To account for the space charge effects due to the emitted current from the sharp tip, we solve the Poisson equation and electron trajectories (through equation of motion) self consistently. The approach is not trivial, and we will describe briefly below. First, the Poisson equation is expressed in the prolate spheroidal coordinates, which gives

$$\nabla^2 V = \frac{\rho}{\varepsilon_0} \tag{3a}$$

and

$$\nabla^2 = \frac{1}{a^2(\sinh^2 u + \sin^2 v)}\left(\frac{\partial^2}{\partial u^2} + \frac{\partial^2}{\partial v^2} + \coth u \frac{\partial}{\partial u} + \cot v \frac{\partial}{\partial v}\right). \tag{3b}$$

In Eq. (3a), the emitted charge density ρ is related to the emitted current density J and also the electrical potential V through the particle and field weighting process as the traditional particle in cell method. The boundary conditions for solving the Poisson equation are

$$V(u,v) = 0 \text{ for } v = v_c, \quad 0 < u < L, \tag{4a}$$

$$V(u,v) = V_g \text{ for } v = \pi/2, \quad 0 < u < L, \tag{4b}$$

$$\frac{\partial V(u,v)}{\partial u} = 0 \text{ for } u = 0, \quad v_c < v < \pi/2, \tag{4c}$$

$$V(u,v) = V_g\left(1 - \frac{\ln(\cot(v/2))}{\ln(\cot(v_c/2))}\right) \text{ for } u = L, \quad v_c < v < \pi/2. \tag{4d}$$

Here, $v = v_c = \theta$ and $v = \pi/2$ define the respective locations of the tip and anode, and L ($>D$) is the size of the computation domain. On the tip axis, the symmetrical boundary condition (Eq. (4c)) is used. The emitted current density J from the tip is confined in an electron emission region bounded by $J(u, v_c) = 0$ for $u > u_0$ at $v = v_c$, where u_0 is a parameter, which defines the size of the emission area $S = \int_0^{u_0}\int_0^{2\pi} h_u h_\varphi \mathrm{d}u\mathrm{d}\varphi$, where $h_u = a\sqrt{\sinh^2(u) + \sin^2(v_c)}$ and $h_\varphi = a\sinh(u)\sin(v_c)$. Equation (4d) is the vacuum electrical potential outside the electron emission region.

To calculate the current density $J(u, v_c)$ emitted from the tip including the space charge effects, we construct an algorithm to solve for the electron trajectories under the influence of both vacuum field and space charge field. We first solve the Laplace equation $\nabla^2 V = 0$, to obtain the vacuum electric field lines as shown in Fig. 1 (yellow line). For first iteration, these vacuum electric fields are used to calculate the electron trajectories by solving the equation of motion $\ddot{z} = eE_z/m$ and $\ddot{r} = eE_r/m$, where $E_z = E_u \mathrm{d}u/\mathrm{d}z + E_v \mathrm{d}v/\mathrm{d}z$ and $E_r = E_u \mathrm{d}u/\mathrm{d}r + E_v \mathrm{d}v/\mathrm{d}r$ are, respectively, the electric field in the z and r directions as shown in Fig. 1. By knowing the electron trajectories, we obtain an initial charge density ρ_{old} as a function of u and v (by depositing the particle onto the grid), which is subsequently used in solving the Poisson equation to obtain a new potential field. This new potential field will give an updated electric field in order to solve equation of motion to obtain new trajectories and also updated charge density ρ^*. In the second iteration, a new charge distribution is constructed by using $\rho_{new} = 0.9 \times \rho_{old} + 0.1 \times \rho^*$ in the algorithm again. The entire process is repeated for 10–20 times until a convergence of ρ is obtained. We call this the Poisson-Trajectory process.

In our model, we consider two types of emission process from the tip: (a) field emission due to sharp tip and (b) unlimited source of electron emission, which is consistent to the original assumption of the 1D CL law, namely, the cathode is always able to supply sufficient electrons (even at low voltage) to drive the electric field at the cathode to be zero.

III. SPACE CHARGE EFFECT ON FIELD EMISSION FROM SHARP TIP

For field emission, we assume the amount of emitted current is governed by the well-known Fowler-Nordheim (FN) law, given by $J_{FN} = AE(u, v_c)^2 \exp[-B/E(u, v_c)]$, where $A = 1.5414 \times 10^{-6}\exp(9.83593/\sqrt{\Phi})/\Phi$, $B = 6.8309 \times 10^9 \Phi^{3/2}$, Φ (=4.7 eV) is the work function,[39] and $E(u, v_c)$ is the surface electric field that is determined self-consistently by solving Eqs. (3) and (4) to include the space charge field. To ensure good accuracy, $E(u, v_c)$ is numerically calculated by an extrapolation process[41,42] based on the electrical potential values at the 3 nearest grid points (in terms of v), which are obtained from the Poisson and trajectory process stated above.

Figure 1 shows the calculated electron trajectories and the electrical potentials with (green and black lines) and without (blue and red lines) the space charge effects, for $R = 50$ nm, $D = 1\,\mu$m, $V_g = 2$ kV, and $u_0 = 0.5$. The field enhancement at the apex is about $\gamma = 9$, which is equivalent to an electric field of about 18 V/nm. It can be seen that the electron trajectories expand due to the space charge effect, and they do not follow the vacuum electric field lines (yellow lines). The equal potential curves including the space charge effect also deviate more from the vacuum case, especially at the region near to the tip apex.

In Fig. 2(a), the convergent process of the current density J (solid line) and also the FN law J_{FN} (dashed line) are presented for comparison. We first use the vacuum electric field $E_0(u, v_c)$ to obtain J_{FN0}, and use $J_{old} = 0.1 \times J_{FN0}$ as the input in the Poisson-Trajectory process to obtain an updated electrical field $E^*(u, v_c)$ and also an updated current density J^* (based on FN law). A new current density is constructed by using a new $J_{new} = 0.9 \times J_{old} + 0.1 \times J^*$, and the entire process is repeated until a convergence is obtained. From the figure, it is clear that the *pure* FN law has overestimated the peak current density at the apex ($u = 0$) by about 25% and the difference becomes negligible at locations far from the apex ($u > 0.2$). Using the calculated J, we plot the normalized charge density ρ in Fig. 2(b), which has a maximum value at the apex because most of the electrons emitted are concentrated near to the apex. The normalized localized current density (in terms of CL law) $\beta = J(0, v_c)/J_{CL}$ at the apex is $\beta = 4.27$. Thus, this finding indicates that the classical CL law is not accurate to predict the maximum current density from a sharp tip if the space charge effect is important.

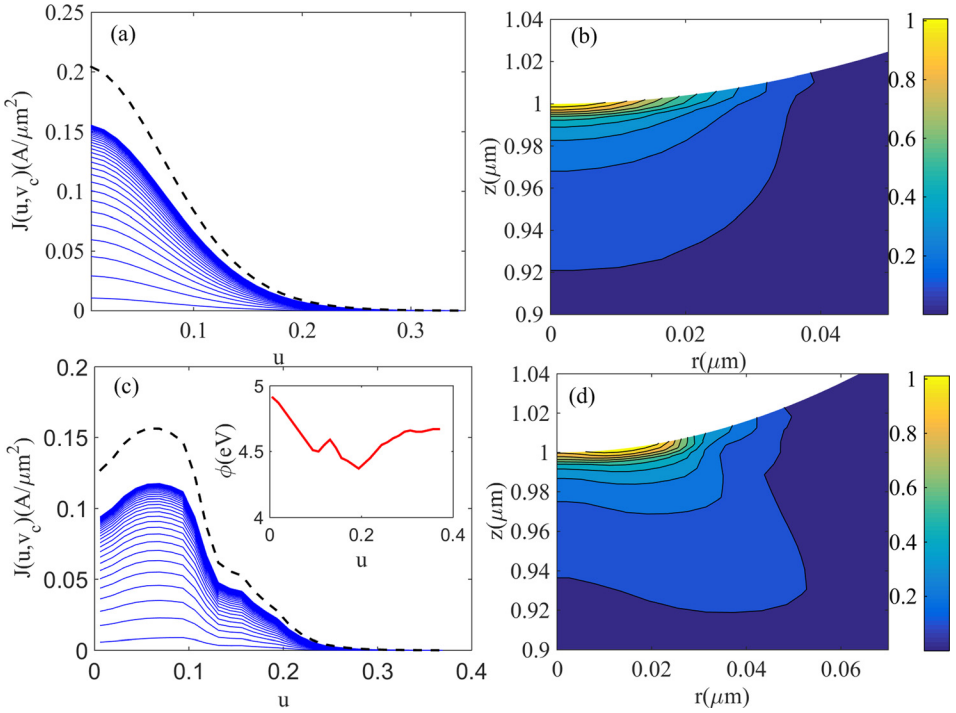

FIG. 2. The calculated profiles of current density $J(u, v_c)$, and charge density $\rho(u, v)$ for a tip with a fixed work function $\Phi = 4.7$ eV [(a) and (b)] and non-uniform work function see inset in (c) and (d) at $V_g = 1$ kV. The non-uniform work function is shown in the inset of Fig. 2(c). The dashed black line is the calculate $J(u, v_c)$ without the space charge effect. The blue line shows the convergence process in the calculation.

For a sharp tip surface, the work function Φ may vary depending on the crystal orientation.[43] By assuming a non-uniform distribution of Φ, based on experimental values [see Fig. 8(c) in Ref. 43], we repeat the calculation of J and ρ for such non-uniform work function case, and the results are shown in Figs. 2(c) and 2(d). The maximal value of J is located at $u = 0.8$ [see Fig. 2(c)], which is neither at the apex ($u = 0$) nor at the position of lowest work function ($u = 0.2$). Thus, we conclude that the maximum charge density distribution [see Fig. 2(d)] is no longer located at the tip apex for such non-uniform work function case.

IV. SPACE CHARGE LIMITED CURRENT

For the unlimited source of electron emission model, we assume that the tip is able to provide a sufficiently high current density in order to push the electric field (at all locations: $u \le u_0$) to be zero, namely,

$$\frac{\partial V(u, v)}{\partial v} = 0 \quad \text{for } v = v_c. \tag{5}$$

Here, a secant method[41] is used in our calculation subjected to the additional boundary condition stated in Eq. (5). Note the model is now independent of the emission process. The Poisson-Trajectory process is used as inner iteration to obtain cathode electric field to fulfill Eq. (5), which defines the required profiles of current density to meet such condition. Once these conditions are met, we define the resulting current density as the space charge limited current for a sharp tip, namely, $J_{SCL}(u, v_c)$, which is a function of u.

Figure 3 shows the normalized $J_{SCL}(u, v_c)$ (in terms of the planar CL law) for (a) various emitting size $u_0 = 0.51$, 0.76, and 1.02 at a fixed $R = 50$ nm, and (b) various radius $R = 50$, 100, and 200 nm at a fixed $u_0 = 0.8$. From the figure, it is clear that $J_{SCL}(u, v_c)$ is sensitive to the geometrical properties of the tip (u_0 and R). Larger emitting area (or higher u_0) will provide more space charge effects and thus smaller current $J_{SCL}(u, v_c)$ is needed. As expected, an enhancement is found to be near to the edge ($u \backsimeq u_0$). This finding is similar to flat cathode (of finite emission area) model observed before.[5,6,41,42] However, the enhancement at the edge is smaller for a sharp tip due to the localized high field at the apex. This implies that localized high value of $J_{SCL}(u, v_c)$ at the apex is more dominant than the edge effect.

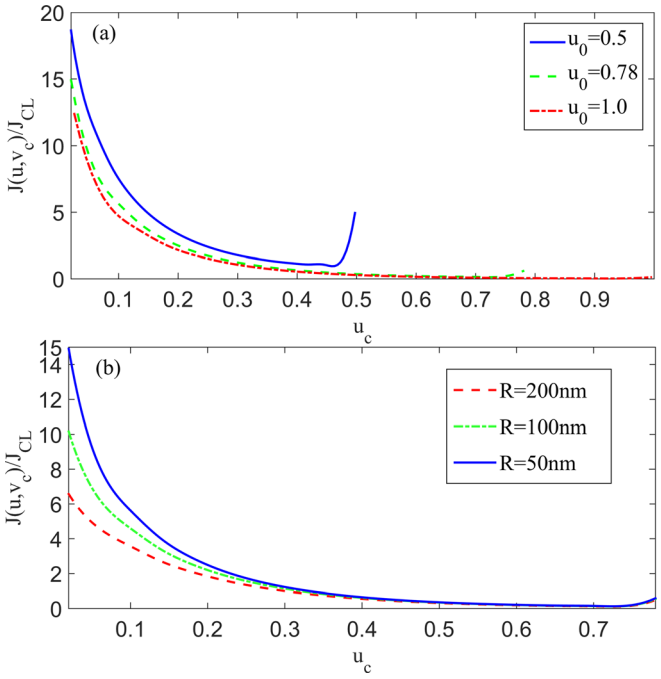

FIG. 3. Spatial variation of the non-uniform protrusive CL law (in terms of the 1D CL law) at fixed $V_g = 1$ kV for (a) various emitting size ($u_0 = 0.51$, 0.76, and 1.02), and (b) various tip radius = 50, 100, and 200 nm at fixed $u_0 = 0.8$.

From Fig. 3(b), we can see that $J_{SCL}(u, v_c)$ increases for smaller R due to higher vacuum electric field, and thus more current is required to reach the SCL condition for smaller R.

In Fig. 4, we study the transition from the pure field emission without the space charge effect (solid line) to the space charge limited current for a sharp tip (square) in two different methods: (a) local current density $J(u, v_c)$ [A/μm^2] (at apex of the tip) and (b) the total current emission I [A] (integrated over the emission area). The calculated results are, respectively, plotted in Figs. 4(a) and 4(b). For completeness, the FN law including space charge effect is also plotted (circle), and the local current density can exceed the value predicted by the space charge limited current density for a sharp tip (square) when the applied voltage is sufficiently large. In terms of the total emitted current, the FN law including space charge effects will always converge to the space charge limited current model for a sharp tip at high enough field, as shown in Fig. 4(b). Thus, we conclude that the space charge limited current model for a sharp tip gives the upper limit of the total emitting current integrated over the entire emitting area, which is independent of the emission process.

In Figs. 5(a) and 5(b), we show that the localized current density on the tip apex as a function of V_g and D, respectively. It is worth noting that the space charge limited current model for a sharp tip has the same scaling of 3/2 power of the applied voltage, similar to the 1D CL law in Eq. (1). However, it is found out that the D^{-2} scaling in the traditional scaling of the 1D CL law ($J_{CL} \propto V_g^{3/2}/D^2$) is no longer valid. The revised scaling for the sharp tip on the tip axis is

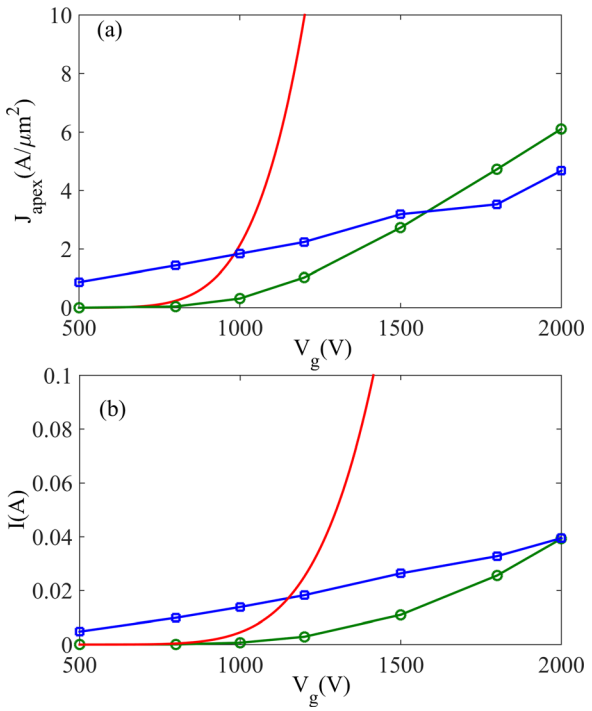

FIG. 4. (a) The tip apex current density J_{apex} and (b) the total current I as a function of V_g for different emission processess: field emission without (solid line) and with (circle) the space charge effects and the protrusive CL law (square). The emission area is varied under different V_g to ensure that the smallest current density (at the edge) is 0.1% of the maximum current density on the tip apex.

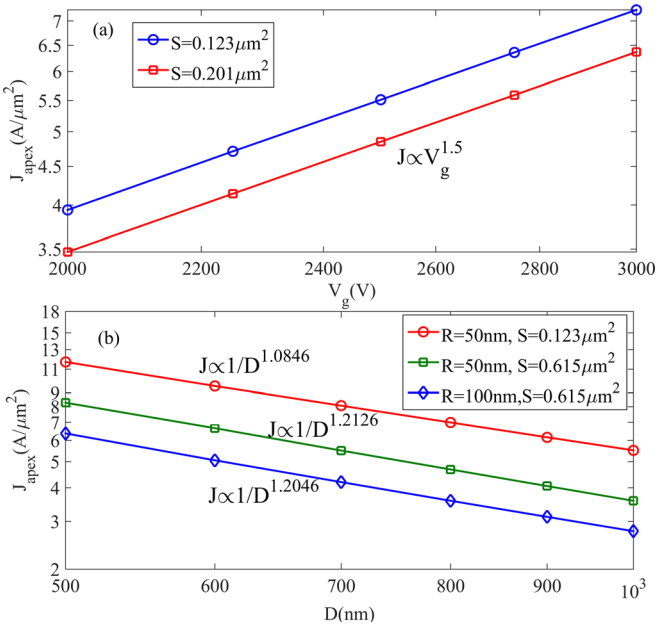

FIG. 5. The scaling of apex current density J_{apex} as (a) a function of V_g (at fixed D) and (b) a function of D (at fixed V_g) for various tip's radius (R) and emission area (S).

$J_{SCL} \propto V_g^{3/2}/D^m$, where m is about 1.1 (for smaller emitting area) to 1.2 (for large emission area). The tip radius ($R = 50$–100 nm) has negligible effect on the scaling proposed here.

V. CONCLUSIONS

In summary, a consistent SCL current model has been constructed to account for high current electron emission from a sharp tip. At the apex, a revised scaling of $J_{SCL} \propto V_g^{3/2}/D^m$ ($m = 1.1$–1.2) is proposed. The effects of non-uniform electron emission and the spatial variation of work function have been studied. The model will be useful to serve as the upper limit or maximum current emission allowed for different cathodes using sharp tip or protrusive structures in various applications.[19–34]

ACKNOWLEDGMENTS

The authors thank Professor Y. Y. Lau, Professor A. Valfells, and Dr. Peng Zhang for very useful discussion. This work was supported by SUTD-ZJU/PILOT/01/2014 and SUTD-MIT IDC Grants (IDG21200106 and IDD21200103). L.K.A. acknowledges the support of AFOAR AOARD Grant (14-2110).

[1]C. D. Child, Phys. Rev. (Ser. I) **32**, 492 (1911).
[2]I. Langmuir, Phys. Rev. **2**, 450 (1913).
[3]J. W. Luginsland, Y. Y. Lau, and R. M. Gilgenbach, Phys. Rev. Lett. **77**, 4668 (1996).
[4]Y. Y. Lau, Phys. Rev. Lett. **87**, 278301 (2001).
[5]R. J. Umstattd and J. W. Luginsland, Phys. Rev. Lett. **87**, 145002 (2001).
[6]A. Rokhlenko and J. L. Lebowitz, Phys. Rev. Lett. **91**, 085002 (2003).
[7]A. Rokhlenko and J. L. Lebowitz, J. Appl. Phys. **110**, 033306 (2011).
[8]Y. Y. Lau, D. Chernin, D. G. Colombant, and P. T. Ho, Phys. Rev. Lett. **66**, 1446 (1991).
[9]L. K. Ang, T. J. T. Kwan, and Y. Y. Lau, Phys. Rev. Lett. **91**, 208303 (2003).

[10]A. Valfells, D. W. Feldman, M. Virgo, P. G. O'Shea, and Y. Y. Lau, Phys. Plasmas **9**, 2377 (2002).
[11]L. K. Ang and P. Zhang, Phys. Rev. Lett. **98**, 164802 (2007).
[12]Y. B. Zhu and L. K. Ang, Appl. Phys. Lett. **98**, 051502 (2011).
[13]Y. B. Zhu, P. Zhang, A. Valfells, L. K. Ang, and Y. Y. Lau, Phys. Rev. Lett. **110**, 265007 (2013).
[14]A. Pedersen, A. Manolescu, and A. Valfells, Phys. Rev. Lett. **104**, 175002 (2010).
[15]P. Jonsson, M. Ilkov, A. Manolescu, A. Pedersen, and A. Valfells, Phys. Plasmas **20**, 023107 (2013).
[16]M. E. Griswold, N. J. Fisch, and J. S. Wurtele, Phys. Plasmas **17**, 114503 (2010).
[17]R. E. Caflisch and M. S. Rosin, Phys. Rev. E **85**, 056408 (2012).
[18]A. Rokhlenko and J. L. Lebowitz, J. Appl. Phys. **114**, 233302 (2013).
[19]*Vacuum Microelectronics*, edited by W. Zhu (Wiley, 2001).
[20]J. H. Booske, Phys. Plasmas **15**, 055502 (2008).
[21]D. R. Whaley, B. M. Gannon, C. R. Smith, C. M. Armstrong, and C. A. Spindt, IEEE Trans. Plasma Sci. **28**, 727 (2000).
[22]J. Petillo, E. M. Nelson, J. F. DeFord, N. J. Dionne, and B. Levush, IEEE Trans. Electron Devices **52**, 742 (2005).
[23]H. Yanagisawa, C. Hafner, P. Dona, M. Klöckner, D. Leuenberger, T. Greber, M. Hengsberger, and J. Osterwalder, Phys. Rev. Lett. **103**, 257603 (2009).
[24]R. Bormann, M. Gulde, A. Weismann, S. V. Yalunin, and C. Ropers, Phys. Rev. Lett. **105**, 147601 (2010).
[25]M. Schenk, M. Kruger, and P. Hommelhoff, Phys. Rev. Lett. **105**, 257601 (2010).
[26]S. Tujino, F. le Pimpec, J. Raabe, M. Buess, M. Dehler, E. Kirk, J. Gobrecht, and A. Wrulich, Appl. Phys. Lett. **94**, 093508 (2009).
[27]L. K. Ang and M. Pant, Phys. Plasmas **20**, 056705 (2013).
[28]M. Gulde, S. Schweda, G. Storeck, M. Maiti, H. K. Yu, A. M. Wodtke, S. Schäfer, and C. Ropers, Science **345**, 200 (2014).
[29]A. H. Zewail and J. M. Thomas, *4D Electron Microscopy* (Imperial College Press, 2009).
[30]R. K. Li and P. Musumeci, Appl. Phys. Rev. **2**, 024003 (2014).
[31]J. Breuer and P. Hommelhoff, Phys. Rev. Lett. **111**, 134803 (2013).
[32]E. A. Peralta, K. Soong, R. J. England, E. R. Colby, Z. Wu, B. Montazeri, C. McGuinness, J. McNeur, K. J. Leedle, D. Walz, E. B. Sozer, B. Cowan, B. Schwartz, G. Travish, and R. L. Byer, Nature **503**, 91 (2013).
[33]R. K. Li, H. To, G. Andonian, J. Feng, A. Polyakov, C. M. Scoby, K. Thompson, W. Wan, H. A. Padmore, and P. Musumeci, Phys. Rev. Lett. **110**, 074801 (2013).
[34]A. Polyakov, C. Senft, K. F. Thompson, J. Feng, S. Cabrini, P. J. Schuck, H. A. Hadmore, S. J. Peppernick, and W. P. Hess, Phys. Rev. Lett. **110**, 076802 (2013).
[35]Y. Y. Lau, Y. F. Liu, and R. K. Parker, Phys. Plasmas **1**, 2082 (1994).
[36]A. Rokhlenko, K. L. Jensen, and J. L. Lebowitz, J. Appl. Phys. **107**, 014904 (2010).
[37]K. L. Jensen, J. Appl. Phys. **107**, 014905 (2010).
[38]K. L. Jensen, D. A. Shiffler, J. J. Petillo, Z. Pan, and J. W. Luginsland, Phys. Rev. Spec. Top. - Accel. Beams **17**, 043402 (2014).
[39]L. H. Pan, T. E. Sullivan, V. J. Peridier, P. H. Cutler, and N. M. Miskovsky, Appl. Phys. Lett. **65**, 2151 (1994).
[40]J. D. Zuber, K. L. Jensen, and T. E. Sullivan, J. Appl. Phys. **91**, 9379 (2002).
[41]J. J. Watrous, J. W. Luginsland, and M. H. Frese, Phys. Plasmas **8**, 4202 (2001).
[42]B. Ragan-Kelley, J. Verboncoeur, and Y. Feng, Phys. Plasmas **16**, 103102 (2009).
[43]H. Yanagisawa, C. Hafner, P. Doná, M. Klöckner, D. Leuenberger, T. Greber, J. Osterwalder, and M. Hengsberger, Phys. Rev. B **81**, 115429 (2010).